J. Hydrol. Hydromech., 70, 2022, 3, 295–307
https://doi.org/10.2478/johh-2022-0021
©2022 Martin Kuban et al., published by Sciendo. This work is licensed under the Creative Commons Attribution-NonCommercial-NoDerivatives 4.0 International Licence.

sciendo Journal of Hydrology and Hydromechanics Institute of Hydrology SAS

The effects of satellite soil moisture data on the parametrization of topsoil and root zone soil moisture in a conceptual hydrological model

Martin Kuban[1*], Juraj Parajka[2,3], Rui Tong[2,3], Isabella Greimeister-Pfeil[2,5], Mariette Vreugdenhil[5,1], Jan Szolgay[1], Silvia Kohnova[1], Kamila Hlavcova[1], Patrik Sleziak[4], Adam Brziak[1]

[1] Slovak University of Technology, Faculty of Civil Engineering, Department of Land and Water Resources Management, Radlinského 11, 810 05 Bratislava, Slovakia.
[2] Centre for Water Resource Systems, TU Wien, Vienna, 1040, Austria.
[3] Institute of Hydraulic Engineering and Water Resources Management, TU Wien, Vienna, 1040, Austria.
[4] Institute of Hydrology, Slovak Academy of Sciences, Dúbravská cesta 9, 84104 Bratislava, Slovakia.
[5] Department of Geodesy and Geoinformation, TU Wien, Vienna 1040, Austria.
[*] Corresponding author. E-mail: martin.kuban@stuba.sk

Abstract: In a previous study, the topsoil and root zone ASCAT satellite soil moisture data were implemented into three multi-objective calibration approaches of the TUW hydrological model in 209 Austrian catchments. This paper examines the model parametrization in those catchments, which in the validation of the dual-layer conceptual semi-distributed model showed improvement in the runoff simulation efficiency compared to the single objective runoff calibration. The runoff simulation efficiency of the three multi-objective approaches was separately considered. Inferences about the specific location and the physiographic properties of the catchments where the inclusion of ASCAT data proved beneficial were made. Improvements were primarily observed in the watersheds with lower slopes (median of the catchment slope less than 15 per cent) and a higher proportion of farming land use (median of the proportion of agricultural land above 20 per cent), as well as in catchments where the runoff is not significantly influenced by snowmelt and glacier runoff. Changes in the mean and variability of the field capacity parameter FC of the soil moisture regime were analysed. The values of FC decreased by 20 per cent on average. Consequently, the catchments' water balance closure generally improved by the increase in catchment evapotranspiration during the validation period. Improvements in model efficiency could be attributed to better runoff simulation in the spring and autumn month. The findings refine recommendations regarding when hydrological modelling could consider satellite soil moisture data added to runoff signatures in calibration useful.

Keywords: ASCAT; TUW model; Soil moisture; Multi-objective calibration; Parameter uncertainty.

INTRODUCTION

The importance of the reliable simulation of soil moisture in rainfall-runoff models is widely recognized since soil moisture, as a significant factor in the mass and energy balance of catchments, acts as a controller in surface and subsurface runoff generation. Recently, the hydrological community has increased efforts to improve its estimation through the assimilation of remotely-sensed soil moisture data into process modelling. Applications include diverse areas such as numerical weather predictions, global and regional climate and land surface model assessments, and the real-time monitoring of drought phenomena. Furthermore, in catchment hydrology, rainfall-runoff modelling and flood forecasting are essential applications benefitting from satellite soil moisture observations. No attempt to review all of these aspects and future prospects will be given here. Instead, this paper focuses on the benefits of using a particular remotely-sensed soil moisture product and its derivatives in rainfall-runoff modelling for Austria.

Concerning recent developments, we refer to evaluations of the use of remotely-sensed soil moisture data and discussions on the potential of estimating soil moisture through remote sensing to be found in Beck et al. (2021), Brocca et al. (2017), De Santis et al. (2021), Fang and Lakshmi (2014), Kim et al. (2019), Liu et al. (2022), Mascaro et al. (2019), Muñoz-Sabater et al. (2016), Tebbs et al. (2016), Wagner et al. (2007).

Passive and active microwave remote sensing has led to progress in the remote observation techniques of soil moisture and have increased the availability of regional and global soil moisture datasets, including a new ASCAT Soil Water Index (SWI) data product, which is tested in this paper (Beck et al., 2021; Kim et al., 2018, 2019; Muñoz-Sabater et al., 2016; Paulik et al., 2014).

Naeimi et al. (2009) presented an improved soil moisture retrieval algorithm based on the TU-Wien method (Wagner et al., 1999) with a series of modifications and a new parametrization (the WAter Retrieval Package 5 (WARP5). This algorithm yielded a more robust and spatially uniform soil moisture product, which is distributed as the soil water index (SWI) by the Copernicus Global Land Service (SWI, 2022).

The results in this paper are based on an experimental SWI data product, which mainly benefits from a new vegetation parameterization of the ASCAT topsoil moisture retrieval algorithm (Steele-Dunne et al., 2021). It includes an improved spatial representation due to the application of a new directional resampling method based on Sentinel-1 Synthetic Aperture Radar (SAR) data (Tong et al., 2021). In addition, it quantifies the moisture conditions at various depths in the soil.

The application of satellite-based soil moisture data in rainfall-runoff modelling is mainly concentrated around three areas: estimation of antecedent soil moisture for the initialization of event-based rainfall-runoff models (e.g., Brocca et al., 2009; Jadidoleslam et al., 2019; Sunwoo and Choi, 2017; Tramblay et al., 2012); assimilation of data for operational forecasting (e.g., Ciupak et al., 2019; Jun et al., 2021; Le et al., 2022; Loizu et al., 2018; Massari et al., 2015; Meng et al., 2017); improvements in the parametrization of continuous (primarily conceptual) hydrological models using multi-objective calibration methods (e.g., Kuban et al., 2021; Li et al., 2018; Olofintoye et. al., 2022; Rajib et al., 2016; Tong et al., 2021; Xiong and Zeng, 2019).

The rationale behind the multi-objective calibration of models, which is also the main topic of this paper, is that even though the representations of soil moisture in the data sources and the models have limitations and are not defined in the same way, connecting these quantities through model parameter calibration helps to reduce the uncertainties associated with estimates of catchment states and outputs (Demirel et al., 2019; Kundu et al., 2017; Nijzink et al., 2018; Parajka et al., 2007; Széles et al., 2020; Tian et al., 2021; Wanders et al., 2014). Efstratiadis and Koutsoyiannis (2010) presented an overview of the development of the methods; for more recent applications, see, e.g., Mostafaie et al. (2018), Bomhof et al. (2019), Adeyeri et al. (2020), Thornton et al. (2021).

In general, previous studies that have calibrated rainfall-runoff models to discharge and soil moisture data have found that using the additional information has typically improved the spatial and temporal patterns of internal soil moisture state variables and fluxes without a clear tendency to improve the runoff simulation.

The study by Parajka et al. (2007) introduced a dual-layer conceptual hydrological HBV - type model and used topsoil moisture observations from an ERS scatterometer. Simulations for discharge-only calibration in 148 Austrian catchments in 1991–2000 yielded higher topsoil moisture values than the scatterometer. In addition, more robust model parameters and states have been reported using both the ERS scatterometer-based soil moisture data and runoff for the model calibrations.

Wanders et al. (2014) addressed the question of which hydrological models' parameters can be identified by calibration with remotely-sensed soil moisture. They concluded that remotely-sensed soil moisture leads to a better simulation of soil moisture content throughout catchments and a better simulation of discharges in upstream areas of the catchments.

Rajib et al. (2016) looked at the relative potential of spatially-distributed surface and root zone soil moisture estimates in calibrating the Soil and Water Assessment Tool (SWAT) model towards improving its hydrological predictability. The multi-objective calibration improved the surface soil moisture simulation, other components of the water balance connected to the surface soil moisture (streamflow, evapotranspiration, and the moisture from the deeper layer remained less affected.

Kundu et al. (2017) used the SWAT model under the hypothesis that multivariate calibration cannot indicate the contribution of improvement in streamflow predictions that is only due to soil moisture. They used raw remotely-sensed surface soil moisture data (soil moisture values not transformed into SWI). The results showed a positive effect of using remotely sensed data also on streamflow. The approach improved the general rainfall-runoff response simulation by introducing delays; however, it could not correct the overall routing effect.

Li et al. (2018) attempted to evaluate the impact of using remotely-sensed soil moisture on discharge predictions at gauged and ungauged locations. Two calibration schemes (multi-objective and discharge only) were compared for a lumped model and a semi-distributed model with only one or several gauges available for calibration. The multi-objective scheme slightly degraded the streamflow predictions at the gauged sites during the streamflow-only calibration. On the other hand, improvements occurred at the same sites in the validation period. In addition, improvements were achieved at the gauged sites not used in the calibration.

Xiong and Zeng (2019) used the SMAP L3 soil moisture product for a multi-objective calibration of a DDRM distributed model. The results showed that changing the weights of the soil moisture in the objective function (from w = 0 to 1.0) led to only slight differences in the performance of the simulation of soil moisture and streamflow. In addition, the streamflow simulation had no apparent advantages over the traditional calibration using the streamflow data only.

Recent advances in satellite remote sensing of soil moisture provide products with improved spatial and temporal resolutions. Tong et al. (2021) showed that using the new ASCAT-SWI root-zone soil moisture product can improve the rainfall-runoff model efficiency of conceptual hydrologic models. Kuban et al. (2021) extended such evaluation and examined the value of both topsoil and root zone soil moisture to calibrate a dual-layer conceptual model. Both studies have analysed a large number (213) of Austrian catchments with the TUW model and indicated good agreement between satellite and modelled soil moisture estimates and the improvement in runoff efficiencies in many catchments. Still, as indicated in Brocca et al. (2017), the conditions when benefits can be achieved from the inclusion of information on satellite soil moisture data to rainfall-runoff modelling (both for data assimilation and model calibration) still need to be further clarified.

This study's main objective is to further assess the results of Kuban et al. (2021) under the diverse physiographic conditions of many Austrian catchments. It intends to analyse the changes in the parametrization of the conceptual TUW model in catchments, where the model performance benefits both in the simulation of soil moisture and runoff from using satellite soil moisture in the multi-objective calibration. In addition, special attention is devoted to the parameterization of the soil moisture regime and the water balance closure.

MATERIALS AND METHODS

Data

From all 209 Austrian catchments calibrated in Kuban et al. (2021), 198 catchments with data available in 1991–2000, representing different physiographical conditions, were used for the model validation. These catchments have been used and also examined within the frame of previous studies such as Viglione et al. (2013), Sleziak et al. (2020), Tong et al. (2021), and represent river basins with no significant anthropogenic influences (Fig. 1). The size of the catchments varies between 13.7 (Micheldorf, Krems River) to 6214 km^2 (Bruck an der Mur unter Műrz, the Mur River). Their average slope varies from 1.74% to 43.91%. The mean annual precipitation is less than 400 mm/year in the east and more than 2500 mm/year in the west. The mean daily air temperature is between −2.83 °C for the Alpine catchments and up to 10.30 °C in the lowland catchments.

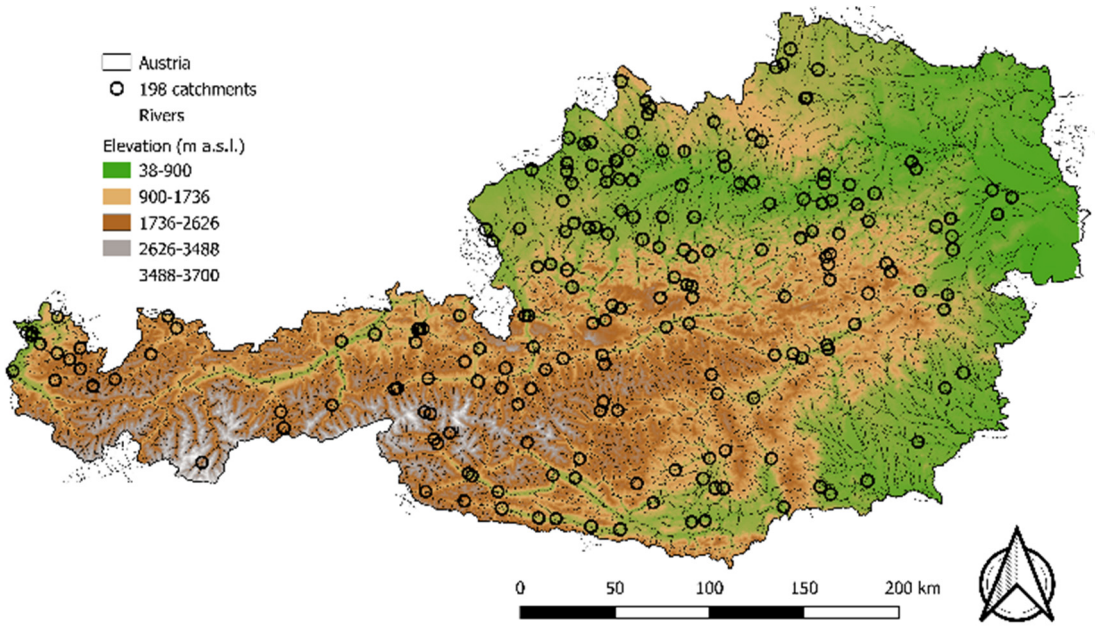


Fig. 1. Location of the 198 catchments selected on the territory of Austria.

Table 1. Selected catchment characteristics for analysed Austrian catchments (Tong, et al. (2021) and Kuban et al. (2021)).

Information	Attribute	Abbrev.	Unit	Min.	Max.	Median
Area	Area	A	km^2	13.7	6214	175.5
Elevation	Mean elevation	MELE	m a.s.l.	353.0	2939.7	1020.8
	Mean slope	SL	%	1.74	43.91	19.36
	Elevation range	ER	m	80	3072	1336
Land use	Forest percentage	FP	%	0.00	94.59	46.9
	Agriculture percentage	AP	%	0.00	92.86	16.3
Soil	Mean saturated hydraulic conductivity	MKS	$cm \cdot day^{-1}$	24.8	327.7	164.0
Climate	Mean annual precipitation	MAP	mm	728.1	2301.8	1281.0
	Mean air temperature	MAT	°C	–2.83	10.30	7.23
	Aridity index	CAI	–	0.18	0.98	0.47
	Duration of days with air temperature below 0 °C	MTL0	%	11.5	62.0	20.4

A digital elevation model with a 500 m spatial resolution was used to derive the topographical characteristics of the catchments analysed. The land cover characteristics have been derived from the CORINE land cover mapping (CLC2006 data set; EEA, 2013; https://land.copernicus.eu/, last access: 5 June 2020). The land cover in Austria mainly consists of agricultural land and meadows in the lowlands and forest and pastures in the medium elevation ranges. Alpine vegetation and bedrock prevail in the catchments in the elevations over 2000 m a.s.l. The percentage of the forest cover is between 0 and 94.6%, and the agricultural soil cover has a range from 0 up to 92.9%.

The soil characteristics are derived from a 1 km global map of hydraulic properties of soil (Zhang et al., 2018). This data set provides the mean and standard deviations of the selected soil hydraulic parameters based on the Kosugi water retention model (Kosugi, 1994, 1996) at a 1 km resolution for the topsoil (0–5 cm).

Hydrological and climate data

The daily runoff data from 198 gauging stations and the period of 1991–2000 used in this study are provided by the Central Hydrographical Bureau (HZB; https://ehyd.gv.at/, last access: 17 March 2021) and the Zentralanstalt für Meteorologie und Geodynamik (ZAMG).

The climatic model inputs (mean daily precipitation and mean daily air temperature) have been derived from the gridded SPARTACUS data set (Hiebl and Frei, 2016, 2017). This data set provides daily 1 km gridded spatial resolution maps covering the whole territory of Austria.

The mean daily potential evaporation was derived from gridded maps of the mean daily air temperature and potential sunshine duration index by using a modified Blaney–Criddle approach by Parajka et al. (2003); for more details and formulae, see, e.g., Kuban et al. (2021).

Table 1 summarizes the selected climate and catchment characteristics used in our study. To better represent the distribution of the altitudes, slopes, and land use in these catchments, the histograms of the mean catchment elevation (MELE), mean catchment slope (SL), forest percentage (FP), and agricultural percentage (AP) are presented in Fig. 2.

ASCAT SWI data

To improve the soil component reactions of the catchments in the calibration of the TUW-dual rainfall-runoff model done in Kuban et al. (2021), an experimental dataset of the Soil Water Index (ASCAT SWI) was used from the experimental version of the ASCAT DIREX Soil Water Index (ASCAT SWI) product similarly as in Tong et al. (2021).

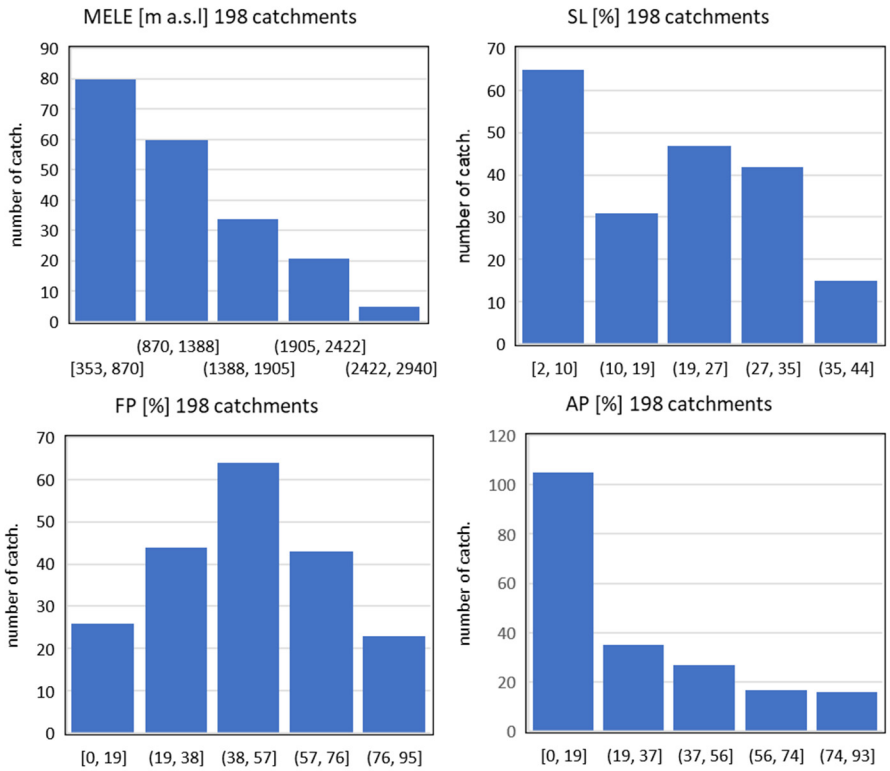


Fig. 2. Histograms of the mean catchment elevation (MELE), mean catchment slope (SL), forest percentage (FP) and agricultural percentage (AP) for 198 Austrian catchments analysed.

The ASCAT SWI product is composed of geophysical parameters, geo-location information, and auxiliary parameters.

The ASCAT SWI dataset available through Copernicus Global Land Service is only available from Metop ASCAT and thus at a 12.5 km spatial resolution. A high resolution SWI is available at 1 km, which assimilates Sentinel-1 soil moisture for the SWI calculation. The disadvantage of this product is that it is only available since 2015 as Sentinel-1 was launched at the end of 2014. As the calibration of the TUW-model needs long time series, an experimental dataset was used which uses static parameters based on Sentinel-1 to obtain SWI at 1 km resolution from Metop ASCAT covering the period 2007–2018.

A number of improvements have been performed in the Metop ASCAT soil moisture product used for SWI calculation tailored to obtain most reliable soil moisture retrievals over Austria. The vegetation parametrization, which corrects for scattering from vegetation was adjusted according to Hahn et al. (2021) and Pfeil et al. (2018), which has shown better soil moisture results for Austria. Second, the soil moisture data was detrended to take out any trends in backscatter that were not related to soil moisture changes but to increased urbanization or land cover change.

The process of disaggregation of the signal from the original 12.5 km to the 500 m sampling consists of a directional resampling method. This method uses the temporal stability of soil moisture, which states that spatial patterns in soil moisture persist over time (Vachaud et al., 1985; Wagner et al., 2008). The temporal stability leads to high temporal correlation between locations and scales. This theory is used to obtain high resolution soil moisture by calculating the directional dependencies (represented by correlation coefficients) between neighbouring regional (12.5 km) and the central, local (0.5 km) scale Sentinel-1 backscatter observations. A local soil moisture signal is calculated based on the regional soil moisture data weighted for their directional dependency (EODC, 2021). This approach provides estimates of the Soil Water Index describing the soil-water content profile on a 0.5 km spatial sampling grid, whereas the effective spatial resolution is believed to be within the range of 5–15 km depending on the location. A key strength of this product is its consistency over long periods of time as its temporal behaviour is only determined by the backscatter measurements acquired by the intercalibrated ASCAT sensors flown board on the Metop -A/B/C, which belongs to the EUMETSAT-operated Metop ASCAT (Advanced Scatterometer) satellite mission.

The Soil Water Index (SWI) is based on an infiltration model describing the relation between the surface, and profile soil moisture as a function of time. It represents the soil moisture content in the first 1 m of the soil in relative units, ranging between the wilting level (0%) and full saturation (100%).

The important parameter for modelling the infiltration into the deeper soil layers is the characteristic time length, called the T-value (the higher the T-value, the smoother the SWI). The T value represents a reduction of the infiltration of the soil moisture dynamics, with higher T values corresponding to a higher degree of reduction so that information on short-term conditions is not lost due to soil moisture dynamics still present in the deeper soil layers, T must therefore be carefully chosen. To avoid losses of short-term soil moisture dynamics, a value of T = 10 days for the ASCAT SWI for the root zone (28–100 cm) and T = 2 for ASCAT SWI for the topsoil zone (3–5 cm) was selected in Kuban et al. (2021).

The ASCAT SWI product used in the model calibration in Kuban et al. (2021) contains data for 2007–2018 for two soil layers (the topsoil and root zone soil layer). The ASCAT data were interpolated from the 500 m × 500 m grid to the same elevation zones as the other input data.

TUW model

The TUW-dual rainfall-runoff model (Viglione and Parajka, 2020), which was used in the research in this paper, is a conceptual lumped or semi-distributed derivative of the well-known HBV model (Bergstrom, 1992; Lindstrom et al., 1997). Catchment runoff is computed from precipitation, air temperature, and potential evapotranspiration inputs on a daily or shorter step basis. The inputs are allowed to vary with the catchment elevation. Consequently, accounting for the soil moisture and snow water equivalent can be performed independently for each elevation zone (200 m altitudinal range in this paper). However, the same model parameters are assumed to apply to all the elevation zones of a catchment. Respecting this limitation, the TUW can be regarded as a semi-distributed conceptual model.

The model consists of snow, soil moisture, and flow-generating modules. It has 18 parameters listed together with their recommended respective ranges, see Table 2. The snow module simulates snow accumulation and melting. It is based on the degree-day concept with two parameters: a degree-day factor (DDF) and a snowmelt temperature parameter (Tm). The snow correction factor (SCF) accounts for the catch deficit of the precipitation gauges during the winter. A threshold temperature interval, i. e., <Tr; Ts>, separates rainfall and snowfall. In the TUW-single version, one storage element represents the runoff generation in the soil moisture module. In the TUW-dual version, two types of soil storage (topsoil and root-zone, see below) are used. Runoff is controlled by the root zone storage, which represents the root zone soil moisture state of the catchment. Three parameters control it, i.e., the maximum root zone soil moisture FC (a parameter that represents the soil moisture state above which evaporation takes place at the potential rate); Lprat, which is the limit for potential evaporation; and BETA, a parameter in the non-linear function that relates runoff generation to the soil moisture in the root-zone.

The runoff generated is routed through an upper and a lower soil reservoir. The excess rainfall enters the upper zone reservoir, which is drained through three outflows. The fast storage coefficient k1 controls the outflow; percolation to the lower zone occurs at the percolation rate (cprec). When the storage state exceeds the threshold (lsuz), additional outflow occurs based on a fast storage coefficient (k0). Finally, the slow storage coefficient (k2) controls the outflow from the lower zone.

The outflow from both reservoirs is then routed by a triangular transfer function representing the runoff routing in the streams, where the croute is a free-scaling parameter.

The TUW-dual model (Parajka et al., 2009) separates the soil module into two layers, i.e., the topsoil and the root zone, respectively. Figure 3 shows the scheme of the dual-layer soil moisture accounting scheme.

The topsoil reservoir is fed by rainfall and snowmelt. If its capacity (Lskin) is exceeded, outflow dQ_{skin} occurs and is divided into two components. The first DQ becomes the direct runoff, and the second dS_s enters the root soil moisture storage. A fraction of the actual evaporation reduces the water in the topsoil moisture reservoir: $AET_{skin} = (1 - \phi)$ AET, where AET is the actual evaporation, and the parameter ϕ subdivides the AET into evaporation from the AET_{main} root and the AET_{skin} top soil layer. The bidirectional moisture flux Q_m connects the top and root soil reservoir. The dual-layer soil moisture accounting scheme introduces three additional parameters for the top soil layer: the fc_skin-field capacity (maximum soil moisture storage of the topsoil layer), α- the transfer parameter, and ϕ – the parameter for a fraction of the actual evapotranspiration. The root zone soil layer maintains the parameters from the single version of TUW. For more information, see Parajka et al. (2009).

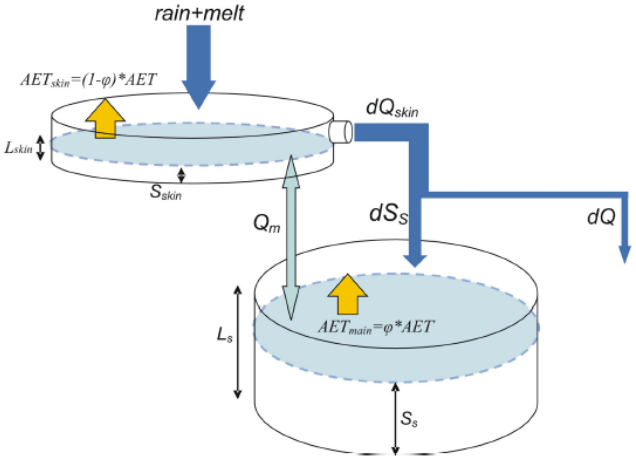


Fig. 3. General scheme of the dual-layer soil moisture accounting scheme in the TUW-dual model (Kuban et al., 2021; Parajka et al., 2009).

Table 2. TUW_dual model parameters with their ranges for 209 Austrian catchments (Kuban et al., 2021; Parajka et al., 2009).

Abbreviation	Description of the model parameters	Range
1. SCF	snow correction factor	(0.9–1.5 [–])
2. DDF	degree day factor	(0.0–5.0 [mm/°C/day])
3. Tr	threshold temperature, above which precipitation is rain	(1.0–3.0 [°C])
4. Ts	threshold temperature, below which precipitation is snow	(–3.0–1.0 [°C])
5. Tm	threshold temperature, above which melting starts	(–2.0–2.0 [°C])
6. Lprat	parameter related to the limit for potential evaporation	(0.0–1.0 [–])
7. FC	field capacity, i.e., maximum soil moisture storage	(0–600 [mm])
8. BETA	the nonlinear parameter for runoff production	(0.0–20.0 [–])
9. k0	storage coefficient for a very fast response	(0.0–2.0 [day])
10. k1	storage coefficient for a fast response	(2.0–30.0 [day])
11. k2	storage coefficient for a slow response	(30.0–250 [day])
12. lsuz	threshold storage state, i.e., the very fast response start if exceeded	(1.0–100 [mm])
13. cperc	constant percolation rate	(0.0–8.0 [mm/day])
14. bmax	maximum base at low flows	(0.0–30.0 [day])
15. croute	free scaling parameter	(0.0–50.0 [day^2 /mm]
16. fc_skin	field capacity, i.e., maximum soil moisture storage of the top skin layer	(0.1–10 [mm])
17. α	transfer parameter	(0.7–0.95 [–])

Calibration

For the sake of completeness, we summarise the single-objective and multi-objective calibration approaches of the TUW-dual model described in Kuban et al. (2021) because the analysis in this paper was set up on the results therein. We intended to examine in a new verification dataset the effects of including the SWI of the topsoil and root zone on the model performance in such types of catchments, where the improved performance of the catchments was achieved in the calibration. Therefore, we performed a multi-objective calibration as combinations composed of the same four single-objective functions (OF) used therein. The function labelled OF_Q was only based on runoff; OF_{Q+SR} was based on the runoff and soil moisture in the root zone; OF_{Q+ST} was based on the runoff and soil moisture in the topsoil layer; and $OF_{Q+SR+ST}$ was based on the runoff and soil moisture both in the root and topsoil layers.

The multi-objective calibration was achieved by the weighted linear combination of the individual single-objective functions OF_Q, OF_{SR}, and OF_{ST} with weights assigned to them in the following combinations:

$$OF_{Q+SR} = OF_Q * w_Q + OF_{SR} * w_{SR} \quad (1)$$

$$OF_{Q+ST} = OF_Q * w_Q + OF_{ST} * w_{ST} \quad (2)$$

$$OF_{Q+SR+ST} = OF_Q * w_Q + OF_{SR} * w_{SR} + OF_{ST} * w_{ST} \quad (3)$$

where w_Q, w_{SR} and w_{ST} were the weights. Based on the analysis of the effect of the weights carried out by Sleziak et al. (2020) and Tong et al. (2021), and following the results of Kuban et al. (2021), in OF_{Q+SR} and OF_{Q+ST}, the values of the weights w_Q, w_{SR} and w_{ST} were set at ½ respectively. In $OF_{Q+SR+ST}$, the values of the weights w_Q, w_{SR}, and w_{ST} were 1/3.

The objective function for the runoff was calculated using an average of the Nash-Sutcliffe coefficient (*NSE*) and the logarithmic *NSE* (Nash and Sutcliffe, 1970):

$$OF = (NSE + \log NSE)/2 \quad (4)$$

$$NSE = 1 - \frac{\Sigma_{i=1}^{n}\left(Qobs(i) - Qsim(i)\right)^2}{\Sigma_{i=1}^{n}\left(Qobs(i) - \bar{Q}obs\right)^2} \quad (5)$$

$$\log NSE = 1 - \frac{\Sigma_{i=1}^{n}\left(\log Qobs(i) - \log Qsim(i)\right)^2}{\Sigma_{i=1}^{n}\left(\log Qobs(i) - \log \bar{Q}obs\right)^2} \quad (6)$$

where $Qsim(i)$ and $Qobs(i)$ are the simulated and observed runoffs at time i; $\bar{Q}obs$ is the average of the flow observed.

The objective function for both soil moisture layers was calculated using the Spearman correlation coefficient between the measured and simulated soil moisture values.

We also measured the efficiency of the TUW-dual model with respect to only the runoff simulation (Runoff Model Efficiency - *RME*):

$$RME = OF \quad (7)$$

The parameter optimization was based on an evolution strategy developed by Storn and Price (1997), termed *differential evolution* (DE). Evolution strategies belong to evolutionary algorithms in which members of the population are represented with floating-point numbers, and the population is transformed over successive generations using arithmetic operations. DE is considered suitable for finding the global optimum of a real-valued function of real-valued parameters. It does not require that the function be either continuous or differentiable. Many implementations exist; here, the **DEoptim** implementation of DE (Ardia and Mullen, 2010), which implements the Differential Evolution algorithm described in Mullen et al. (2011), was used.

RESULTS

Improvement in the runoff simulation in the 1991–2000 validation period

The results of the parameter calibrations for the single calibration (Q) and three multi-objective calibration variants considering the ASCAT SWI data (Q+ST, Q+SR, Q+ST+SR) and the 2007–2014 calibration period were published in Kuban et al. (2021), where 209 Austrian catchments were divided into Alpine and Lowland catchments. The single multi-objective calibration approach (Q) represents calibration only on runoff, the variants of the multi-objective calibration approach represent: calibration on runoff and topsoil moisture (Q+ST), calibration on runoff and root soil moisture (Q+SR), and calibration on runoff, and both topsoil and root soil moisture (Q+ST+SR).

In this study, we analysed the model performance to simulate runoff in the validation period of 1991–2000 by using the model parameters from all the above variants of the single and multi-objective model calibration approaches. We did not divide the catchments into Alpine and Lowland catchments but only into catchments where the multi-objective calibration approach using the ASCAT SWI data improved or did not improve the values of runoff model efficiency RME. 198 basins with available data were used for the 1991–2000 validation.

Figure 4 displays the catchments where the multi-objective calibration approach for all the three multi-objective calibration variants (Q+ST, Q+SR, Q+ST+SR) improved the RME in the validation period. The figure shows that the catchments with the improvement in RME are mainly located in the lowland regions and are not completely identical for the individual variants of the multi-objective calibration.

For the multi-calibration variant Q+ST an improvement in the RME was indicated in 44 catchments, for the multi-calibration variant Q+SR in 44 catchments, and for the multi-calibration variant Q+ST+SR in 34 catchments. The medians of the RME in these catchments are presented in Table 3.

Table 3 shows that the multi-objective calibration variant Q+ST improved the runoff model efficiency in 44 catchments, with the improvement in the RME medians from 0.715 to 0.722. The multi-objective calibration variant Q+SR improved the runoff model efficiency in 44 catchments, with the improvement in the RME medians from 0.702 to 0.722. Finally,

Table 3. Medians of RME in the catchments where the multi-objective calibration approach (Q+ST, Q+SR, and Q+ST+SR) improved the runoff simulation in the 1991–2000 validation period. Q represents calibration on runoff, Q+ST calibration on runoff and top zone soil moisture, Q+SR calibration on runoff and root zone soil moisture, Q+ST+SR calibration on runoff, and both topsoil and root zone soil moisture.

Number of catchments, RME	Single calibration approach (Q)	Multi-objective calibration approach (Q+ ST, Q+SR, Q+ST+SR)
44 catchments	Q	Q+ST
RME	0.715	0.722
44 catchments	Q	Q+SR
RME	0.702	0.721
34 catchments	Q	Q+ST+SR
RME	0.67	0.693

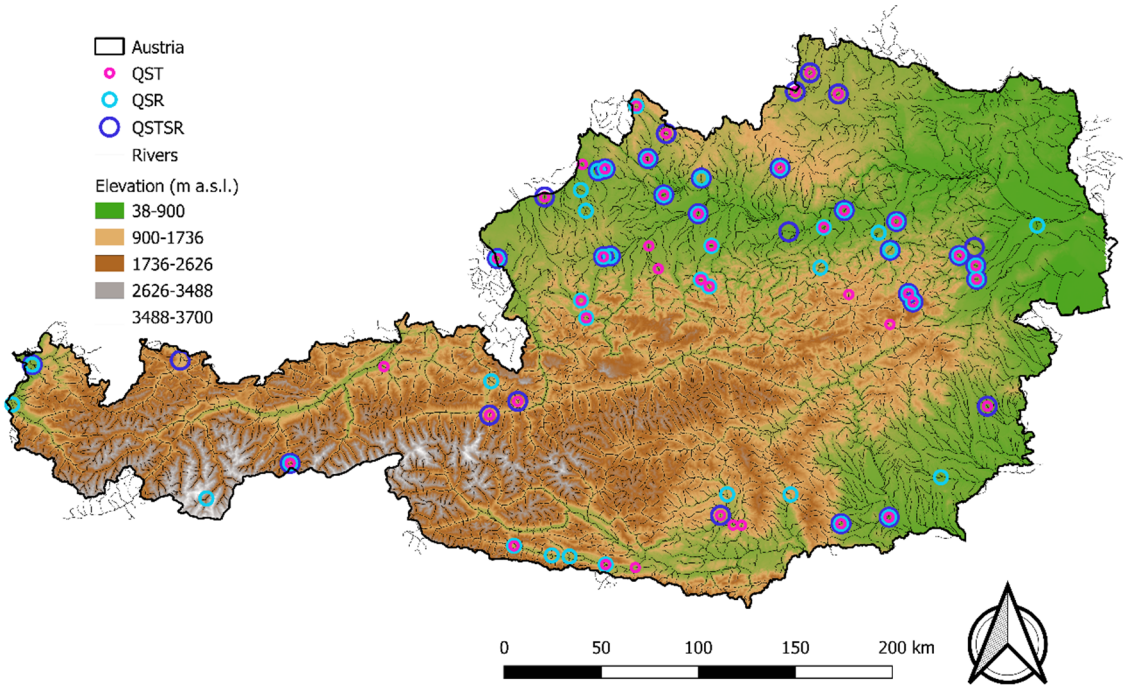


Fig. 4. Location of the catchments with improved RME in the 1991–2000 validation period. Improved catchments for individual multi-objective calibration variants Q+ST, Q+SR, and Q+ST+SR are marked with a different colour. Q+ST represents calibration on runoff and top zone soil moisture, Q+SR calibration on runoff and root zone soil moisture, Q+ST+SR calibration on runoff, and both topsoil and root zone soil moisture.

Table 4. The medians of catchment characteristics for the improved and unimproved catchments in the 1991–2000 validation period: [+] improved catchments, [–] catchments without any improvement. A is the catchment area, MELE is the mean catchment elevation, SL is the mean catchment slope, FP is the forest percentage, AP is the agricultural percentage, MAP is the mean annual precipitation, and MTLT0 is the duration of days with air temperatures below 0 °C. The values which most specified the differences between the catchment characteristics of improved and unimproved catchments are marked in bold.

Medians of the catchment characteristics for 198 catchments										
198	[%]	[Num.]	[+/–]	A	MELE	SL	FP	AP	MAP	MTLT0
Q+SR	22%	44	improved	223.2	**761.0**	**13.6**	54.4	**23.7**	1216.2	0.17
Q+ST	22%	44		239.4	**849.7**	**13.2**	57.6	**21.9**	1173.2	0.18
Q+ST+SR	17%	34		183.5	**719.2**	**8.5**	52.1	**39.2**	1077.1	0.17
Q+SR	78%	154	unimproved	170.2	**1178.1**	**22.1**	46.4	**14.4**	1307.4	0.22
Q+ST	78%	154		165.1	**1176.9**	**22.0**	45.5	**14.2**	1307.4	0.22
Q+ST+SR	83%	164		168.1	**1178.1**	**22.7**	46.4	**13.4**	1326.0	0.22
Medians of 198 catchments				178.3	1036	19.48	46.7	16.1	1277.7	0.20

the multi-objective calibration variant Q+ST+SR improved the RME in 34 catchments, with the improvement in the RME medians from 0.69 to 0.693.

The improvement in the RME was similar for the multi-objective calibration variants Q+ST and Q+SR. If both soil moisture products are used in the model calibration (Q+ST+SR), the number of improved catchments is slightly smaller.

We subsequently analysed as to whether the improvement in the runoff model efficiencies is dependent on a catchment's properties and whether it is possible to define the predominant catchment characteristics for these improvements. For all the improved and unimproved catchments and all the calibration variants, we present the medians of the selected catchment characteristics in Table 4: catchment area (A), mean elevation (MELE), mean slope (SL), forest percentage (FP), agricultural percentage (AP), mean annual precipitation (MAP), and duration of days with air temperatures below 0 °C (MTLT0).

The improvement in RME can be seen in the catchments with a lower mean elevation (MELE) and a lower mean slope (SL); the medians of MELE range from 719 to 850 m a.s.l., and the medians of SL are within a range of 8.5 to 13.6%. In the catchments without any improvement in the RME, the medians of MELE are about 1178 m a.s.l., and the medians of SL are about 22%. Behind the mean catchment elevations and the catchment slopes, among the dominant catchment characteristics influencing the runoff model efficiency belongs land use, especially the agricultural percentage (AP). It can be seen that the improved catchments have a higher AP compared with the catchments without any improvement in RME. In the improved catchments, the medians of the agricultural percentage (AP) vary from 22 to 39%, while in the catchments without any improvement, the AP varies from 13 to 14%.

Comparison of the model parameters from the single and multi-objective calibrations

Within our analysis of changes in the model parameters from the multi-objective calibration approach compared to the single calibration approach, we identified the most significant changes in the parameter of the field capacity (FC), which is the most sensitive parameter for simulating soil moisture in the root zone. Therefore, in this part of the study, we compare the behaviour of this parameter from single and multi-objective calibration in improved catchments. Finally, we try to specify how and in which type of catchments the multi-objective calibration changed the values of FC, which could lead to an improvement of the RME in these catchments.

In Figure 5, we selected only those catchments where the improvement of the RME values was detected for the three multi-objective calibration variants and marked the changes in the FC values.

Boxplots of the FC values in Fig. 6 confirm that the distribution of the FC parameter in the improved catchments is different when we use the single or the multi-objective calibration approach. While the median of FC is approximately 200 mm from a single calibration, the medians of FC are about 150 mm for all three multi-objective calibration variants.

Finally, in Table 5, we can see the amounts and characteristics of the improved catchments with an increase or decrease in FC. The bold type indicates the catchment characteristics with the most specified differences between the groups of increased or decreased FC.

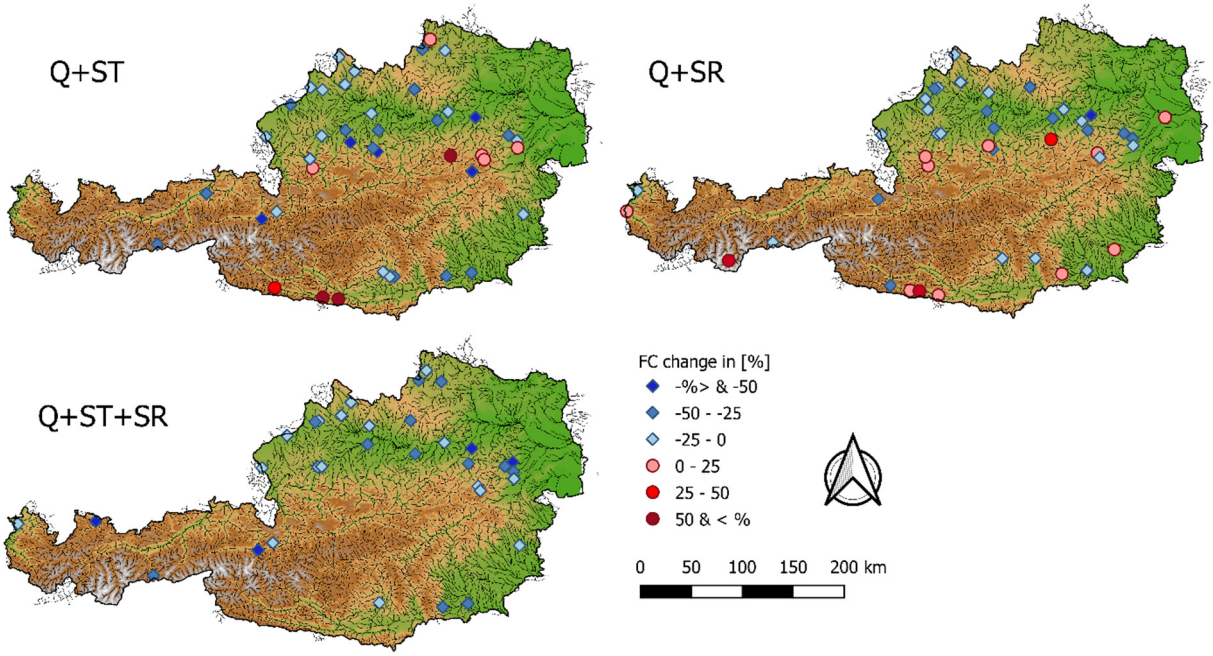


Fig. 5. Catchments with a decrease (in %) in FC (blue) and with an increase in FC (red) for the three multi-objective calibration variants (Q+ST, Q+SR, and Q+ST+SR) versus the single calibration. Q+ST represents calibration on runoff and topsoil moisture, Q+SR calibration on runoff and root soil moisture, Q+ST+SR calibration on runoff, and both topsoil and root soil moisture. Catchments with a decrease in FC are marked with several shades of blue, and catchments with an increase in FC with several shades of red.

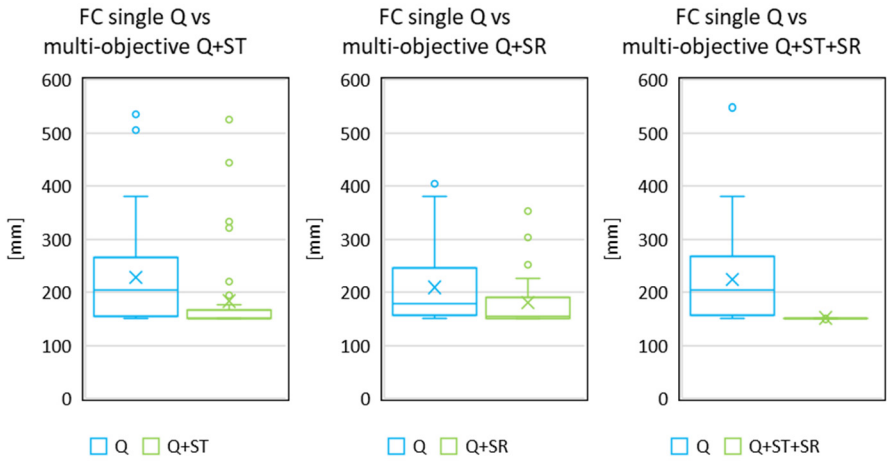


Fig. 6. Boxplots of FC from the single and multi-objective calibration approaches (Q, Q+ST, Q+SR, and Q+ST+SR) for the improved catchments by the multi-objective calibration approach. Q represents calibration on runoff, Q+ST calibration on runoff and topsoil moisture, Q+SR calibration on runoff and root soil moisture, Q+ST+SR calibration on runoff, and both topsoil and root soil moisture. FC quartiles from the single calibration (Q) are marked in blue, and FC quartiles from the multi-objective calibration approach (Q+ST, Q+SR, Q+ST+SR) are marked in green.

Table 5. The characteristics of the catchments where the multi-objective approach increases the FC (+) and decreases the FC (–); the values which most specified the differences between the groups of FC+ and FC- are marked in bold.

	Number of catchments	Medians of FC [%] +/–	MELE m a.s.l.	SL %	FP %	AP %	CAI –	MTLT0 %
Q+ST	9	20.59	**987.28**	**19.73**	67.20	**10.88**	0.41	19
Q+SR	13	11.65	**952.95**	**22.27**	61.18	**8.80**	0.41	19
Q+ST+SR	0	–	**–**	**–**	–	**–**	–	–
Q+ST	35	–26.32	**771.51**	**10.84**	53.30	**23.53**	0.63	18
Q+SR	31	–16.97	**714.31**	**10.84**	52.37	**32.01**	0.61	16
Q+ST+SR	34	–23.36	**730.16**	**8.73**	52.80	**39.13**	0.64	17

Table 6. Comparison of the percentage of catchments where the water balance closure was improved using the multi-objective against the single calibration approach.

Multi-objective approach	% of catch. with the **improvement in water balance closure**	Multi-objective approach with the **decrease in the FC**	% of catch. with the **improvement in water balance closure**	Multi-objective approach with the **increase in the FC**	% of catch. with the **improvement in water balance closure**
Q+ST (44 catch)	60%	Q+ST (35catch)	69%	Q+ST (9 catch)	40%
Q+SR (44 catch.)	60%	Q+SR (31 catch.)	61%	Q+SR (13 catch.)	62%
Q+ST+SR (34 catch.)	77%	Q+ST+SR (34 catch.)	77%	Q+ST+SR (0 catch.)	0%

Table 7. Percentage of the catchments with the improvement in the long-term mean monthly simulated runoff using the multi-objective approaches.

Multi-objective approach	Percentage of the improved catchments in long-term mean monthly runoff											
	Jan	Feb	Mar	Apr	May	Jun	Jul	Aug	Sep	Oct	Nov	Dec
Q+ST (44 catch.)	**55**	**57**	**57**	**61**	48	43	45	34	39	**59**	**64**	**55**
Q+SR (44 catch.)	50	**55**	**61**	**61**	43	50	39	34	45	**52**	**48**	**52**
Q+ST+SR (34 catch.)	**56**	**65**	**62**	**59**	**59**	**56**	38	26	32	**65**	**62**	**56**
Q+ST FC- (35 catch.)	**60**	**57**	**66**	**63**	43	43	43	37	40	**60**	**66**	**60**
Q+SR FC-(31 catch.)	**61**	**58**	**58**	**58**	39	48	42	39	**52**	**61**	**52**	**55**
Q+ST+SR FC-(34 catch.)	**56**	**65**	**62**	**59**	**59**	**56**	38	26	32	**65**	**62**	**56**
Q+ST FC+ (9 catch.)	33	**56**	22	**56**	**67**	44	**56**	22	33	**56**	**56**	33
Q+SR FC+(13 catch.)	23	46	**62**	**62**	**54**	**54**	31	23	31	31	38	**46**
Q+ST+SR FC+ (0 catch.)	0	0	0	0	0	0	0	0	0	0	0	0

The table shows that in most of the improved catchments (for Q+SS = 35/44, for Q+SR = 31/44, and for Q+SS+SR = 34/34 of the catchments), we detected a decrease in the FC values. The decrease in the median of FC for the multi-objective calibration variant Q+ST was –26.32%, for the Q+SR variant, it was –16.97%, and for the Q+ST+QR variant, it was –23.36%. The FC values decreased in the catchments with similar characteristics compared to those with an improvement in the values of RME. These are the catchments with a lower mean elevation (medians of 714–771 m a.s.l.), a lower slope of the terrain (medians of 9–11%), and a higher percentage of agricultural lands (medians of 24–39%). Conversely, the increase in the FC values was detected in the catchments with a higher mean elevation (medians of 953–987 m a.s.l.), a higher slope of the terrain (medians of 20–22%), and a lower percentage of agricultural lands (medians of 9–11%). The increase in the median of FC for the multi-objective calibration variant Q+ST was +20.59%, for the Q+SR variant, it was +11.65%, and for the Q+ST+QR variant, no catchments with an increase in FC were detected.

Changes in water balance closure and the long-term mean monthly runoff

In this part of the study, we compared the water balance closure and the simulated long-term mean monthly runoff in the improved catchments using parameters from the single and multi-objective calibration approaches with ASCAT SWI data. We wanted to see whether using of a multi-objective approach would give comparable or better results of the water balance closure for the improved catchments. The analysis was done for the 1991–2000 validation period.

The comparison of the percentage of catchments where the water balance closure was improved using the multi-objective calibration approach is summarised in Table 6. From the results presented, we can conclude that the improvement in water balance closure was in 60% of catchments using the multi-objective calibration approach Q+ST or Q+SR and in 77% using the combination of Q+ST+SR compared to the single calibration approach. We could also see that the catchments' water balance closure generally improved by the increase in catchment evapotranspiration during the validation period. Furthermore, when we divide the catchments according to the increase and decrease in FC values, we could observe that for the decreased FC values, the improvement in using the multi-objective calibration approach was more significant than for the catchment with increased FC values.

Next the comparison of the improvement in the long-term mean monthly simulated runoff using the multi-objective approach was also evaluated for the individual months and is presented in Table 7. The evaluation showed that in more than 50% of catchments, the improvements in the long-term mean monthly simulated runoff occurred in the spring, late autumn and winter months, mainly from October to April. However, for the multi-objective approach (Q+ST+SR), the percentage of improved catchments was almost higher and contained the months of May and June.

When we split the catchments according to the increase and decrease in FC values, we could observe that for the increased FC values, the improvement in the long-term mean annual runoff simulation using the multi-objective approach was higher than for the catchment with increased FC values.

Finally, we can conclude that any improvement in the simulated runoff and water balance closure using ASCAT SWI data is mainly noticeable in the winter and spring months and vice versa; decreases in the simulation efficiency occurred in the driest summer and autumn months. This may be related to the ASCAT SWI product providing moderately distorted data for very dry soil (EODC, 2021). It has also been confirmed that better improvements in the simulations can be expected in the flat river basins compared to the hilly types, as well as in river basins with a lower average slope.

DISCUSSION

The issue of improving hydrological model performance with the inclusion of remotely-sensed soil moisture data in multi-objective model calibration had been investigated in several studies. Practical experience shows that by preferring specific properties of a system, single-objective calibrations may lead to increased errors in some characteristics of other properties (Mostafaie et al., 2018). Multi-objective calibration allows for a compromise between different objectives when defining a set of system parameters (Monteil et al., 2020). Wanders et al. (2014) concluded that remotely-sensed soil moisture leads to a better simulation of soil moisture content throughout the catchments and a better simulation of discharges in upstream areas. The analysis by Rajib et al. (2016) follows that while the multi-objective calibration improved the topsoil soil moisture simulation, other components of the water balance connected to topsoil soil moisture (streamflow, evapotranspiration, and the deeper layer moisture) remained less affected. Kubáň et al. (2021) estimated that the efficiency of the model to simulate soil moisture with the parameters calibrated only for the runoff was rather low in the Alpine catchments in Austria but the combination of soil moisture and runoff in the multi-objective calibration approach improved the soil moisture simulation in the majority of the catchments.

Unlike previous studies implementing remotely-sensed soil moisture data with a focus mainly on improving the soil moisture simulation, in our study we only focused on estimating an improvement in the runoff simulation in the validation period. From the analysis of runoff model efficiency (RME) in 198 Austrian catchments representing different physiographical conditions, it can be concluded that the catchments with an improvement in RME are mainly located in the lowland regions. We detected an improvement in RME in the catchments with a lower mean elevation and a lower mean slope. Additionally, the percentage of agricultural land is a dominant catchment characteristic influencing the runoff model efficiency; the improved catchments have a higher agricultural land percentage than the catchments without any improvement in the RME. These findings are consistent with Kuban et al. (2021), where the validation of the model parameters from the multi-calibration approaches with the ASCAT SWI data was provided for 189 Austrian catchments in the 2015–2016 validation period.

For all three multi-objective calibration variants, a decrease in the FC was detected in most of the improved catchments. While the median of FC is approximately 200 mm from the single calibration in the improved catchments, the medians of FC are about 150 mm for all three multi-objective calibration variants. This finding can indicate an overestimation of the soil moisture in the root zone using the single calibration approach. The analysis also shows that the FC values decreased in the catchments with similar characteristics compared to those with an improvement in the RME. These are catchments with a lower mean elevation, a lower terrain slope, and a higher percentage of agricultural lands. Conversely, an increase in the FC values was detected in the catchments where the RME values did not improve or had deteriorated.

Improvements in the simulated mean monthly runoff and water balance closure using the ASCAT SWI data were mainly noticeable in the winter and spring months and vice versa; decreases in the simulation efficiency occurred in the driest summer and autumn months. These facts may be related to the ASCAT SWI product providing moderately distorted data for very dry soil (EODC, 2021). It has also been confirmed that better improvements in the simulations can be expected in the flat river basins compared to the hilly types, as well as in river basins with a lower average slope.

Our study showed moderate to significant improvements by including satellite data in streamflow simulations but deteriorated performance was also noted. Thus, we can confirm the conclusions from the review of the scientific literature in Brocca et al. (2017). They reported that the conditions when benefits can be achieved from including information on satellite soil moisture in runoff modelling (both for data assimilation and model calibration) still need to be further refined. For the future, they recommended approaching the problem from both sites. We can confirm their conclusion that there is a need to tailor the satellite data and to request modellers to adapt models for the use of satellite data.

CONCLUSIONS

In this study, we analysed the TUW-dual model efficiency to simulate runoff in the validation period of 1991–2000 by using the model parameters from the single and the multi-objective calibration approach considering the ASCAT-SWI data (published in Kuban et al. (2021)). The values of runoff model efficiency (RME) were estimated in 198 Austrian catchments situated in different physiographic and climate conditions. An improvement in the RME for the multi-objective calibration approach has been indicated in around 20% of the catchments, mainly located in the lowland regions. These were the catchments with a lower mean elevation, a lower mean slope and a higher agricultural land percentage than the catchments without any improvement in the RME. We can conclude that the catchments where an improvement in the RMEs using the ASCAT SWI data is expected are situated in the lowland regions with a high percentage of agricultural lands (medians higher than 20%), a lower mean elevation (medians lower than 850 m a.s.l.), and lower terrain slopes (medians lower than 15%).

In analysing the model parameters from the single and multi-objective calibration approach, we detected the most significant changes in the parameter of field capacity (FC). The FC values decreased in most of the improved catchments, and a decrease in the medians of FC for the multi-objective calibration approach in improved catchments was around 50 mm. In the improved catchments, for the multi-objective calibration variant Q+ST, a decrease in the FC has been detected in 80% of the catchments, for the variant of Q+SR in 70% of the catchments and for the variant Q+ST+SR in 100% of the catchments.

Finally, we compared the simulated long-term mean monthly runoff, and water balance closure in the improved catchments using parameters from the single and multi-objective

calibration approaches. We can conclude that improvements in the long-term mean monthly runoff using the ASCAT SWI data were in more than 50% of catchment in average, and noticeable in the winter and spring months and vice versa; decreases in the simulation efficiency occurred in the driest summer and autumn months. What is concerning water balance closure the improvement was in 60% of catchments using the multi-objective calibration approach Q+ST or Q+SR and in 77% using the combination of Q+ST+SR compared to the single calibration approach. Furthermore, for the decreased FC values, the improvement in using the multi-objective calibration approach was more significant.

Acknowledgement. This work was supported by the Slovak Research and Development Agency under Contract No. No. APVV-19-0340 and the VEGA Grant Agency No. 1/0632/19. At the same time we would like to acknowledge the support from the Stefan Schwarz grant of the Slovak Academy of Sciences. This work has been supported in the frame of the AlpCarp Project No. 2019-10-15-002 under the bilateral program "Action Austria – Slovakia, Cooperation in Science and Education". The authors thank the agency for its research support. This work was also supported by the Austrian Science Funds (FWF) as part of the Vienna Doctoral Program on Water Resource Systems (DK W1219-N28), the Austrian Research Promotion Agency (FFG) through the BMon project (Contract No. 866031) in the acknowledgments. The authors also like to thank to the project ZMENPAK, within the project for the support of the young scientists at Slovak University of Technology.

REFERENCES

Adeyeri, O.E., Laux, P., Arnault, J., Lawin, A. E., Kunstmann, H., 2020. Conceptual hydrological model calibration using multi-objective optimization techniques over the transboundary Komadugu-Yobe basin, Lake Chad Area, West Africa. Journal of Hydrology: Regional Studies, 27, 100655. DOI: 10.1016/j.ejrh.2019.100655

Ardia, D., Mullen, K., 2010. DEoptim: Differential Evolution Optimization in R. R package version 2.0-4, URL http://CRAN.R-project.org/package=DEoptim

Beck, H.E., Pan, M., Miralles, D.G., Reichle, R.H., Dorigo, W. A., Hahn, S. et al., 2021. Evaluation of 18 satellite- and model-based soil moisture products using in situ measurements from 826 sensors. Hydrol. Earth Syst. Sci., 25, 1, 17–40. DOI: 10.5194/hess-25-17-2021

Bergstrom, S., 1992. The HBV model - its structure and applications. Report No. 4. Swedish Meteorological and Hydrological Institute.

Bomhof, R.H., Gärtner, F.R., Stiggelbout, A.M., et al., 2019. Key components of shared decision making models: a systematic review. BMJ Open, 9 12, e031763. DOI: 10.1136/bmjopen-2019-031763

Brocca, L., Melone, F., Moramarco, T., Morbidelli, R., 2009. Antecedent wetness conditions based on ERS scatterometer data. J. Hydrol., 2009, 364, 73–87.

Brocca, L., Ciabatta, L., Massari, C., Camici, S., Tarpanelli, A., 2017. Soil moisture for hydrological applications: Open questions and new opportunities. Water, 9, 2, 140. DOI: 10.3390/w9020140

Ciupak, M., Ozga-Zielinski, B., Adamowski, J., Deo, R. C., Kochanek, K., 2019. Correcting satellite precipitation data and assimilating satellite-derived soil moisture data to generate ensemble hydrological forecasts within the HBV Rainfall-Runoff Model. Water, 11, 10, 2138. DOI: 10.3390/w11102138

Demirel, M.C., Özen, A., Orta, S., Toker, E., Demir, H.K., Ekmekcioğlu, Ö. et al., 2019. Additional value of using satellite-based soil moisture and two sources of groundwater data for hydrological model calibration. Water, 11, 10, 2083. https://doi.org/10.3390/w11102083

De Santis, D., Biondi, D., Crow, W.T., Camici, S., Modanesi, S., Brocca, L., Massari, C., 2021. Assimilation of satellite soil moisture products for river flow prediction: An extensive experiment in over 700 catchments throughout Europe. Water Resources Research, 57, e2021WR029643. https://doi.org/10.1029/2021WR029643

Efstratiadis, A., Koutsoyiannis, D., 2010. One decade of multiobjective calibration approaches in hydrological modelling: a review. Hydrological Sciences Journal, 55, 1, 58–78. DOI: 10.1080/02626660903526292

EODC, 2021. Product User Manual ASCAT DIREX SWI 0.5 km, v1.0.

Fang, B., Lakshmi, V., 2014. Soil moisture at watershed scale: Remote sensing techniques. J. Hydrol., 516, 258–272.

Hahn, S., Wagner, W., Steele-Dunne, S., Vreugdenhil, M., Melzer, T., 2021. Improving ASCAT soil moisture retrievals with an enhanced spatially variable vegetation parameterization. IEEE Transactions on Geoscience and Remote Sensing, 59, 10, 8241–8256. https://doi.org/10.34726/1622

Hiebl, J., Frei, C., 2016. Daily temperature grids for Austria since 1961 – Concept, creation and applicability. Theor. Appl. Clim., 124, 161–178.

Hiebl, J., Frei, C., 2017. Daily precipitation grids for Austria since 1961 – Development and evaluation of a spatial dataset for hydroclimatic monitoring and modelling. Theor. Appl. Clim., 132, 327–345.

Jadidoleslam, N., Mantilla, R., Krajewski, W.F., Goska, R., 2019. Investigating the role of antecedent SMAP satellite soil moisture, radar rainfall and MODIS vegetation on runoff production in an agricultural region. Journal of Hydrology, 579, 124210. DOI: 10.1016/j.jhydrol.2019.124210

Jun, S., Park, J.H., Choi, HJ., Lee, Y.H., Lim, Y.J., Boo, K.O., Kang, H.S., 2021. Impact of soil moisture data assimilation on analysis and medium-range forecasts in an Operational Global Data Assimilation and Prediction System. Atmosphere, 12, 1089. https://doi.org/10.3390/atmos12091089

Kim, H., Parinussa, R., Konings, A. G., Wagner, W., Cosh, M. H., Lakshmi, V. et al., 2018. Global-scale assessment and combination of SMAP with ASCAT (active) and AMSR2 (passive) soil moisture products. Remote Sensing of Environment, 204, 260–275. DOI: 10.1016/j.rse.2017.10.026

Kim, S., Zhang, R., Pham, H., Sharma, A., 2019. A review of satellite-derived soil moisture and its usage for flood estimation. Remote Sens. Earth Syst. Sci., 2, 4, 225–246. DOI: 10.1007/s41976-019-00025-7

Kuban, M., Parajka, J., Tong, R., Pfeil, I., Vreugdenhil, M., Sleziak, P., Adam, B., Szolgay, J., Kohnová, S., Hlavcova, K., 2021. Incorporating advanced scatterometer surface and root zone soil moisture products into the calibration of a Conceptual Semi-Distributed Hydrological Model. Water, 13, 3366. https://doi.org/10.3390/w13233366

Kundu, D., Vervoort, R.W., van Ogtrop, F.F., 2017. The value of remotely sensed surface soil moisture for model calibration using SWAT. Hydrol. Process., 31, 15, 2764–2780. DOI: 10.1002/hyp.11219

Kosugi, K., 1994. Three-parameter lognormal distribution model for soil water retention. AGU, https://doi.org/10.1029/93WR02931

Kosugi, K., 1996. Lognormal distribution model for unsaturated soil hydraulic properties. Water Resources Research, 32, 2697–2703.

Le, M.H., Nguyen, B.Q., Pham, H.T., Patil, A., Do, H.X., Ramsankaran, R.A.A.J., Bolten, J.D., Lakshmi, V., 2022. Assimilation of SMAP products for improving streamflow simulations over tropical climate region – Is spatial information more important than temporal information? Remote Sensing, 14, 1607. https://doi.org/10.3390/rs14071607

Li, Y., Grimaldi, S., Pauwels, V., Walker, R.N., Jeffrey P., 2018. Hydrologic model calibration using remotely sensed soil moisture and discharge measurements: The impact on predictions at gauged and ungauged locations. Journal of Hydrology, 557, 897–909. DOI: 10.1016/j.jhydrol.2018.01.013

Lindstrom, G., Barbro J., Magnus, P., Marie, G., Sten, B., 1997. Development and test of the distributed HBV-96 hydrological model. Journal of Hydrology, 201, 1–4, 272–288. https://doi.org/10.1016/S0022-1694(97)00041-3

Liu, W., Wang, J., Xu, F., Li, C., Xian, T., 2022. Validation of four satellite-derived soil moisture products using ground-based in situ observations over Northern China. Remote Sensing, 14, 6, 1419. DOI: 10.3390/rs14061419

Loizu, J., Massari, C., Álvarez-Mozos, J., Tarpanelli, A., Brocca, L., Casalí, J., 2018. On the assimilation set-up of ASCAT soil moisture data for improving streamflow catchment simulation. Advances in Water Resources, 111, 86–104. DOI: 10.1016/j.advwatres.2017.10.034

Mascaro, G., Ko, A., Vivoni, E.R., 2019. Closing the loop of satellite soil moisture estimation via scale invariance of hydrologic simulations. Scientific Reports, 9, 1, 16123. DOI: 10.1038/s41598-019-52650-3.

Massari, C., Brocca, L., Tarpanelli, A., Moramarco, T., 2015. Data assimilation of satellite soil moisture into rainfall-runoff modelling: A complex recipe? Remote Sensing, 7, 9, 11403–11433. DOI: 10.3390/rs70911403

Meng, S., Xie, X., Liang, S., 2017. Assimilation of soil moisture and streamflow observations to improve flood forecasting with considering runoff routing lags. Journal of Hydrology, 550, 568–579. DOI: 10.1016/j.jhydrol.2017.05.024

Monteil, C., Zaoui, F., Le Moine, N., Hendrickx, F., 2020. Multi-objective calibration by combination of stochastic and gradient-like parameter generation rules – the caRamel algorithm. Hydrol. Earth Syst. Sci., 24, 3189–3209. https://doi.org/10.5194/hess-24-3189-2020

Mostafaie, A., Forootan, E., Safari, A., Schumacher, M., 2018. Comparing multi-objective optimization techniques to calibrate a conceptual hydrological model using in situ runoff and daily GRACE data. Comput. Geosci., 22, 3, 789–814. DOI: 10.1007/s10596-018-9726-8

Mullen, K.M., Ardia, D., Gil, D.L., Windover, D., Cline, J., 2011. DEoptim: An R Package for Global Optimization by Differential Evolution. Journal of Statistical Software, 40, 6, 1–26. https://doi.org/10.18637/jss.v040.i06

Muñoz-Sabater, J., Al Bitar, A., Brocca, L., 2016. Soil moisture retrievals based on active and passive microwave data: State-of-the-art and operational applications. In: Petropoulos, G.P., Srivastava, P., Kerr, Y. (Eds.): Satellite Soil Moisture Retrievals: Techniques and Applications. Elsevier: Amsterdam, The Netherlands, 18, pp. 351–378.

Naeimi, V., Scipal, K., Bartalis, Z., Hasenauer, S., Wagner, W., 2009. An improved soil moisture retrieval algorithm for ERS and METOP scatterometer observations. IEEE Trans. Geosci. Remote Sensing, 47, 7, 1999–2013. DOI: 10.1109/TGRS.2008.2011617

Nash, J.E., Sutcliffe, J.V., 1970. River flow forecasting through conceptual models part I – A discussion of principles. Journal of Hydrology, 10, 3, 282–290. DOI: 10.1016/0022-1694(70)90255-6

Nijzink, R.C., Almeida, S., Pechlivanidis, I.G., Capell, R., Gustafssons, D., Arheimer, B. et al., 2018. Constraining conceptual hydrological models with multiple information sources. Water Resour. Res., 54, 10, 8332–8362. DOI: 10.1029/2017WR021895

Olofintoye, O., Ayanshola, A., Salami, A., Idrissiou, A., Iji, J., Adeleke, O., 2022. A study on the applicability of a Swat model in predicting the water yield and water balance of the Upper Ouémé catchment in the Republic of Benin. Slovak Journal of Civil Engineering, 30, 1, 57–66. https://doi.org/10.2478/sjce-2022-0007

Parajka, J., Merz, R., Blöschl, G., 2003. Estimation of daily potential evapotranspiration for regional water balance modeling in Austria. In: 11th International Poster Day and Institute of Hydrology Open Day "Transport of Water, Chemicals and Energy in the Soil – Crop Canopy – Atmosphere System". Slovak Academy of Sciences, Bratislava, pp. 299–306.

Parajka, J., Merz, R., Blöschl, G., 2007. Uncertainty and multiple objective calibrations in regional water balance modeling: a case study in 320 Austrian catchments. Hydrol. Process., 21, 435–446. DOI: 10.1002/hyp.6253

Parajka, J., Naeimi, V., Blöschl, G., Komma, J., 2009. Matching ERS scatterometer based soil moisture patterns with simulations of a conceptual dual layer hydrologic model over Austria. Hydrol. Earth Syst. Sci., 13, 259–271. https://doi.org/10.5194/hess-13-259-2009

Paulik, C., Dorigo, W., Wagner, W., Kidd, R., 2014. Validation of the ASCAT Soil Water Index using in situ data from the International Soil Moisture Network. International Journal of Applied Earth Observation and Geoinformation, 30, 1–8. DOI: 10.1016/j.jag.2014.01.007

Pfeil, I., Vreugdenhil, M., Hahn, S., Wagner, W., Strauss, P., Blöschl, G., 2018. Improving the seasonal representation of ASCAT soil moisture and vegetation dynamics in a temperate climate. Remote Sensing, 10, 1788. https://doi.org/10.3390/rs10111788

Rajib, M.A., Venkatesh, M., Zhiqiang, Y., 2016. Multi-objective calibration of a hydrologic model using spatially distributed remotely sensed/in-situ soil moisture. Journal of Hydrology, 536, 2016, 192–207. ISSN 0022-1694. https://doi.org/10.1016/j.jhydrol.2016.02.037

Storn, R., Price, K., 1997. Differential evolution – A simple and efficient heuristic for global optimization over continuous spaces. Journal of Global Optimization, 11, 341–359. https://doi.org/10.1023/A:1008202821328

Sunwoo, W., Choi, M., 2017. Robust initial wetness condition framework of an event-based rainfall–runoff model using remotely sensed soil moisture. Water, 9, 2, 77. DOI: 10.3390/w9020077

Sleziak, P., Szolgay, J., Hlavčová, K., Danko, M., Parajka, J., 2020. The effect of the snow weighting on the temporal stability of hydrologic model efficiency and parameters. Journal of Hydrology, 583, 124639. ISSN 0022-1694. https://doi.org/10.1016/j.jhydrol.2020.124639

Steele-Dunne, S.C., Hahn, S., Wagner, W., Vreugdenhil, M., 2021. Towards including dynamic vegetation parameters in the EUMETSAT H SAF ASCAT soil moisture products. Remote Sensing, 13, 1463. https://doi.org/10.3390/rs13081463

SWI, 2022. https://land.copernicus.eu/global/products/swi

Széles, B., Parajka, J., Hogan, P., Silasari, R., Pavlin, L., Strauss, P., Blöschl, G., 2020. The added value of different

data types for calibrating and testing a hydrologic model in a small catchment. Water Resources Research, 56, 10, e2019WR026153. DOI: 10.1029/2019WR026153

Tebbs, E., Gerard, F., Petrie, A., De Witte, E., 2016. Emerging and potential future applications of satellite-based soil moisture products. In: Petropoulos, G.P., Srivastava, P., Kerr, Y. (Eds.): Satellite Soil Moisture Retrievals: Techniques and Applications. Elsevier: Amsterdam, The Netherlands, 19, pp. 379–400.

Thornton, J.M., Mariethoz, G., Brauchli, T.J., Brunner, P., 2021. Efficient multi-objective calibration and uncertainty analysis of distributed snow simulations in rugged alpine terrain. Journal of Hydrology, 598, 126–241. DOI: 10.1016/j.jhydrol.2021.126241

Tian, S., Renzullo, L.J., Pipunic, R.C., Lerat, J., Sharples, W., Donnelly, C., 2021. Satellite soil moisture data assimilation for improved operational continental water balance prediction. Hydrol. Earth Syst. Sci., 25, 4567–4584. https://doi.org/10.5194/hess-25-4567-2021, 2021

Tong, R., Parajka, J., Salentinig, A., Pfeil, I., Komma, J., Széles, B. et al., 2021. The value of ASCAT soil moisture and MODIS snow cover data for calibrating a conceptual hydrologic model. Hydrol. Earth Syst. Sci., 25, 1389–1410. DOI: 10.5194/hess-25-1389-2021

Tramblay, Y., Bouaicha, R., Brocca, L., Dorigo, W., Bouvier, C., Camici, S., Servat, E., 2012. Estimation of antecedent wetness conditions for flood modelling in northern Morocco. Hydrol. Earth Syst. Sci., 16, 4375–4386.

Vachaud, G., Passerat De Silans, A., Balabanis, P., Vauclin, M., 1985. Temporal stability of spatially measured soil water probability density function. Soil Sci. Soc. Am. J., 49, 4, 822–828. DOI: 10.2136/sssaj1985.03615995004900040006x

Viglione, A., Parajka, J., 2020. Lumped/Semi-Distributed Hydrological Model for Education Purposes. http://CRAN.R-project.org/package=TUWmodel, published 2020-02-26, License: GPL-2 | GPL-3, accessed 07/04/2022.

Viglione, A., Parajka, J., Rogger, M., Salinas, J.L., Laaha, G., Sivapalan, M., Blöschl, G., 2013. Comparative assessment of predictions in ungauged basins – Part 3: Runoff signatures in Austria. Hydrol. Earth Syst. Sci., 17, 2263–2279, https://doi.org/10.5194/hess-17-2263-2013

Wagner, W., Lemoine, G., Rott, H., 1999. A method for estimating soil moisture from ERS scatterometer and soil data. Remote Sens. Environ., 70, 2, 191–207.

Wagner, W., Blöschl, G., Pampaloni, P., Calvet, J.C., Bizzarri, B., Wigneron, J.P., Kerr, Y., 2007. Operational readiness of microwave remote sensing of soil moisture for hydrologic applications. Hydrol. Res., 38, 1–20.

Wagner, W., Pathe, C., Doubkova, M., Sabel, D., Bartsch, A., Hasenauer, S., Blöschl, G., Scipal, K., Martínez-Fernández, J., Löw, A., 2008. Temporal stability of soil moisture and radar backscatter observed by the advanced synthetic aperture radar (ASAR). Sensors, 8, 1174–1197. https://doi.org/10.3390/s80201174

Wanders, N., Bierkens, M.F.P., de Jong, S.M., de Roo, A., Karssenberg, D., 2014. The benefits of using remotely sensed soil moisture in parameter identification of large-scale hydrological models. Water Resour. Res., 50, 8, 6874–6891. DOI: 10.1002/2013WR014639

Xiong, L., Zeng, L., 2019. Impacts of introducing remote sensing soil moisture in calibrating a distributed hydrological model for streamflow simulation. Water, 11, 4, 666. DOI: 10.3390/w11040666

Zhang, Y., Schaap, M.G., Zha, Y., 2018. A high-resolution global map of soil hydraulic properties produced by a hierarchical parameterization of a physically based water retention model. Water Res., 54, 9774–9790.

Received 6 July 2022
Accepted 23 July 2022